



# Dynamic Amplification of Light Signals in Photorefractive Ferroelectric Liquid Crystalline Mixtures

Takeo Sasaki\*, Satoshi Kajikawa, and Yumiko Naka

DOI: 10.1039/b000000x [DO NOT ALTER/DELETE THIS TEXT]

The photorefractive effect in photoconductive ferroelectric liquid crystals that contain photoconductive chiral compounds was investigated. Terthiophene compounds with chiral structures were chosen as the photoconductive chiral compounds, and they were mixed with an achiral smectic C liquid crystal. The mixtures exhibit the ferroelectric chiral smectic C phase. The photorefractivity of the mixtures was investigated by two-beam coupling experiments. It was found that the ferroelectric liquid crystals containing the photoconductive chiral compound exhibit a large gain coefficient of over  $1200 \text{ cm}^{-1}$  and a fast response time of 1 ms. Real-time dynamic amplification of an optical image signal of over 30 fps using the photorefractive ferroelectric liquid crystal was demonstrated.

## 1 Introduction

The photorefractive effect in ferroelectric liquid crystals has been attracting significant interest.<sup>1</sup> The photorefractive effect is a phenomenon that allows for the formation of holographic images within a material; it provides the potential to realize dynamic holograms by recording holograms as a change in the refractive index of a medium.<sup>2,3</sup> The characteristic phenomenon of the photorefractive effect is asymmetric energy exchange in two-beam coupling that can be used to coherently amplify signal beams; therefore, the photorefractive effect has the potential to be used in a wide range of optical technologies similar to a transistor in electrical circuits. Optically transparent materials that show both photovoltaic and electro-optic effects can exhibit the photorefractive effect.

Several photorefractive materials have been developed, including inorganic ferroelectric photoconductive crystals, organic photoconductive crystals, photoconductive nonlinear optical organic polymers, amorphous organic photoconductive materials, photoconductive amphiphilic compounds, and photoconductive liquid crystals (LCs).<sup>4-6</sup> Organic materials in particular have attracted significant interest in

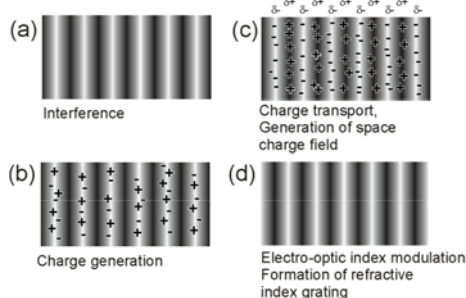


Fig. 1. Schematic illustration of the mechanism of the photorefractive effect. (a) Two laser beams interfere in the photorefractive material; (b) charge generation occurs in the bright areas of the interference fringes; (c) electrons are trapped at trap sites in the bright areas, holes migrate by diffusion or drift in the presence of an external electric field and generate an internal electric field between the bright and dark positions; and (d) the refractive index of the corresponding area is altered by the internal electric field that is generated.

this context since 1994, because they exhibit large photorefractivity and shorter response times.<sup>6</sup>

5 The photorefractive effect induces a change in the refractive index by a mechanism that involves both photovoltaic and electro-optic effects (Fig. 1). When two laser beams  
10 interfere in an organic photorefractive material, charge generation occurs at the bright positions of the interference fringes. At the same time, an electric field is usually applied to the material. The generated charges diffuse or drift within the material. The mobilities of  
15 the positive and negative charges are different in most organic materials, so that a charge separated state is formed. The charge with higher mobility diffuses over a longer distance than the charge with lower mobility; therefore,  
20 while the low mobility charge stays in the bright areas, the high mobility charge moves to the dark areas. The bright and dark positions of the interference fringes are thus charged with opposite polarities, and an internal electric field (space charge field) is formed in the area between the bright and dark positions. The refractive index of the area between the bright and dark positions is changed through the electro-optic effect. Thus, a refractive index grating (in other words, a hologram) is formed.

30 A high electric field of 10–50 V/ $\mu\text{m}$  is usually applied to a polymer film, in addition to the internal electric field, to obtain photorefractivity. The polymer material is typically 100  $\mu\text{m}$  thick, so that the voltage necessary to achieve photorefractivity is 1–5 kV, which is comparable to the breakdown voltage of the polymer film. This electric field is necessary to increase the charge generation efficiency. One class of  
35 materials that exhibits high photorefractivity is glassy photoconductive polymers doped with high concentrations of D- $\pi$ -A chromophores, in which the donor and acceptor groups are attached to a  $\pi$ -conjugate system.<sup>6,7</sup> A multiplex hologram has been demonstrated using a photorefractive polymer film during the development of a 3D display,<sup>8,9</sup> and clear 3D images were recorded in the film. However, the slow  
40 response (ca. 100 ms) and high electric field (30–50 V/ $\mu\text{m}$ ) required to activate the photorefractive effect in polymer materials require improvement.

The photorefractive effect in LCs has been investigated previously.<sup>7</sup> LCs are basically liquid, so they can be easily driven by a low electric field. LCs are classified into several groups, the most well known of which are nematic and smectic LCs.  
45 Nematic LCs are used in liquid crystal displays (LCDs), whereas smectic LCs are very viscous and are thus seldom utilized in practical applications. Nematic LCs were first used as a photorefractive LC and large photorefractivity was obtained with the application of an electric field of only a few volts per micrometer.<sup>10</sup> The photorefractive effect has been reported in surface-stabilized ferroelectric liquid

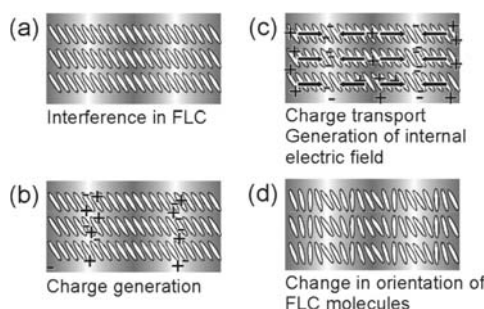


Fig. 2. Schematic illustration of the photorefractive effect in the FLCs. (a) Two laser beams interfere in the SS-state of the FLC/photoconductive compound mixture; (b) charge generation occurs in the bright areas of the interference fringes; (c) electrons are trapped at trap sites in the bright areas, holes migrate by diffusion or drift in the presence of an external electric field to generate an internal electric field between the bright and dark positions; and (d) the orientation of the spontaneous polarization vector (i.e., orientation of mesogens in the FLCs) is altered by the internal electric field.

crystals (SS-FLCs) doped with a photoconductive compound.<sup>14-15</sup> Ferroelectric liquid crystals (FLCs) belong to the class of smectic LCs that have a layered structure.<sup>16,17</sup> FLCs exhibit a chiral smectic C phase (SmC\*) that possesses a helical structure. In order to observe ferroelectricity in the FLCs, they must be formed into thin films.<sup>14</sup>

The thickness of the film needs to be a few micrometers. When an FLC is sandwiched between glass plates to form a film a few micrometers thick, the helical structure of the SmC\* phase uncoils and a surface-stabilized state (SS-state) is formed in which spontaneous polarization (Ps) appears.

For display applications, the thickness of the film is typically 2  $\mu\text{m}$ . In such thin films, FLC molecules can align in only two directions, which is the SS-state, and the alignment direction of the FLC molecules changes according to the direction of the spontaneous polarization. When an alternating electric field is applied to the SS-FLC, the FLC molecules show a continuous switching motion. The electrical switching response time of FLCs is typically shorter than 1 ms. The direction of the spontaneous polarization is governed by the applied electric field, which gives rise to a change in properties according to the direction of polarization. Thus, when an internal electric field is created in an SS-FLC material, the direction of spontaneous polarization is changed by the field.

Figure 2 shows a schematic illustration of the mechanism of the photorefractive effect in FLCs. When laser beams interfere in a mixture of an FLC and a photoconductive compound, charge separation occurs between the bright and dark positions and internal electric fields are produced. The internal electric field alters the direction of spontaneous polarization in the area between the bright and dark positions of the interference fringes, which induces a periodic change in the orientation of the FLC molecules. This is different from the processes that occur in other organic photorefractive materials, in that the molecular dipole rather than the bulk polarization responds to the internal electric field. The switching of FLC molecules is due to the response of bulk polarization and is thus extremely fast. We have investigated the photorefractive effect in commercially available FLCs mixed with a photoconductive dopant and that of FLC mixtures comprising liquid crystalline compounds and photoconductive chiral dopants. The FLC mixtures containing photoconductive chiral dopants exhibited a large photorefractive effect. In this study, the composition of the FLC mixture was further optimised and application to optical signal amplification was demonstrated.

### 1.2 Characteristics of the Photorefractive Effect

As mentioned earlier, a change in the refractive index via the photorefractive effect occurs in the areas between the bright and dark positions of the interference fringes

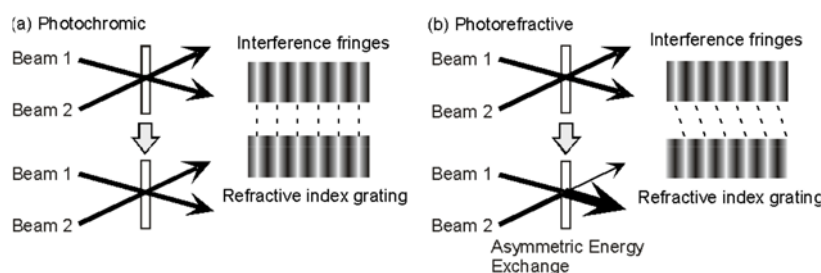


Fig. 3. (a) Photochromic grating and (b) photorefractive grating.

so that the phase of the resulting index grating is shifted from that of the interference fringes. A characteristic of the photorefractive effect is that the phase of the refractive index grating is  $\pi/2$ -shifted from the interference fringes under conditions where one of the photogenerated charges does not move from the bright position. When the material is photochemically active and is not photorefractive, then a photochemical reaction occurs at the bright areas, and a refractive index grating with the same phase as that of the interference fringes is formed [Fig. 3(a)]. The interfering laser beams are diffracted by this grating; however, when the intensities of the interfering beams are equal, the apparent transmitted intensities of the laser beams do not change, because the diffraction is symmetric. Beam 1 is diffracted in the direction of beam 2 and beam 2 is diffracted in the direction of beam 1. However, if the material is photorefractive, then the phase of the refractive index grating is shifted from that of the interference fringes and this affects the propagation of the two beams. Beam 1 is energetically coupled with beam 2 for two laser beams, and consequently, the apparent transmitted intensity of beam 1 increases while that of beam 2 decreases [Fig. 3(b)]. This phenomenon where one beam is amplified by another beam is termed asymmetric energy exchange in a two-beam coupling experiment.<sup>2,3</sup> The photorefractivity of a material is confirmed by the occurrence of this asymmetric energy exchange, which has the potential for a vast variety of optical applications.

## 2 Experimental

### 2.1 Samples

Compared to nematic LCs, FLCs are more crystalline than liquid, so that the preparation of fine FLC films requires sophisticated techniques.<sup>16,17</sup> It is very difficult to obtain a uniformly aligned, defect-free SS-FLC using a single FLC compound. Consequently, mixtures of several LC compounds are usually used to obtain fine SS-FLC films. An FLC mixture is composed of the base LC, which is a mixture of several LC compounds, and a chiral compound. The chiral compound introduces a helical structure to the LC phase through supramolecular interactions. To utilize a FLC as a photorefractive material, photoconductive compounds must be added to the FLC. However, the introduction of such non-LC compounds to the FLC often hinders the formation of a uniformly aligned SS state. Thus, appropriate design of the photoconductive compounds is crucial.

The structures of the LC compounds, the electron acceptor trinitrofluorenone (TNF) and the photoconductive chiral compounds used in this study are shown in Fig. 4. The photoconductive chiral compounds were synthesized as described in a previous paper.<sup>11</sup> TNF was obtained from Tokyo Kasei Co. The smectic C (SmC) liquid crystal used in this study was a 1:1:2 mixture of 5-Octyl-2-(4-octyloxyphenyl) pyrimidine (8PP8), 2-(4-Decyloxyphenyl)-5-octyl pyrimidine (8PP10), and 2-(4-hexyloxy)-5-octyl pyrimidine (8PP6). 8PP8, 8PP10, and

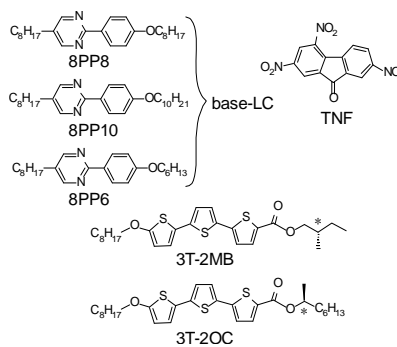


Fig. 4. Structures of the smectic LCs (8PP8, 8PP10 and 8PP6), photoconductive chiral dopants (3T-2MB and 3T-2OC) and the sensitizer TNF.

8PP6 were obtained from Wako Chemicals Co., and were purified by recrystallization from a mixture of methanol and ethyl acetate solution.

5 The mixing ratio of 8PP8, 8PP10, and 8PP6 was set to 1:1:2 because the 1:1:2 mixture exhibits the SmC phase over the widest temperature range. Hereafter, the 1:1:2 mixture

10 of 8PP8, 8PP10, and 8PP6 is referred to as the base LC. The concentration of TNF was 0.1 wt.%. The base LC, TNF, and photoconductive chiral compound

15 were dissolved in dichloroethane, and the solvent was evaporated. The mixture was then dried in vacuum at room temperature for one week. The samples were subsequently injected into a 10- $\mu\text{m}$ -gap glass cell equipped with 1  $\text{cm}^2$  ITO electrodes and a polyimide alignment layer (LX-1400, Hitachi Chemicals Co.) for the measurements. The samples were heated to a temperature where the FLCs exhibit the

20 isotropic phase. The samples were then gradually cooled to ambient temperature at a rate of 0.1  $^{\circ}\text{C}/\text{min}$ . This process is necessary for preparing uniformly aligned FLC samples.

## 2.2 Measurements

Phase transition temperatures were determined using differential scanning calorimetry

25 (DSC; DSC822, Mettler) and microscopic observations (FP-80, FP-82, Mettler; BX-50 polarizing microscope, Olympus). Spontaneous polarization ( $P_s$ ) was measured by the triangular waveform voltage method (10  $V_{p-p}$ , 100 Hz). The photorefractive effect was measured in a two-beam coupling experiment. A linearly polarized beam from a diode-pumped solid state laser (DPSS laser, Spectra Physics, Cyan-PC13689, 488 nm,

30 continuous wave or Oxxious, 473S-50-COL-PP, 473 nm, continuous wave) was divided in two by a beam splitter; the two beams were then interfered in the sample film. A  $p$ -polarized beam was used in most of the experiments in this study. The laser intensity was 1  $\text{mW}/\text{cm}^2$  for each beam (1 mm diameter). The orientation of the rubbing direction and the beam incidence plane are shown in Fig. 5. The incident beam

35 angles to the glass plane were  $40^{\circ}$  and  $60^{\circ}$ . Each interval of the interference fringe was 1.87  $\mu\text{m}$ . The sample was maintained at 25  $^{\circ}\text{C}$  using a thermo-controller (DB1000, Chino Co.). An electric field in the range of 0 to 10  $\text{V}/\mu\text{m}$  was applied to the sample from a regulated DC power supply (Kenwood DW36-1), and the change in the transmitted beam intensity was monitored by photodiodes (ET-2040, Electro-Optics

40 Technology, Inc.) and recorded by an oscilloscope. The formation time for the refractive index grating in the FLC was measured based on the simplest single-carrier model of photorefractivity,<sup>4,5</sup> in which the gain transient is exponential. The rising signal of the two-beam coupling was fitted by a single exponential function.

## 3 Results and discussions

### 45 3.1 POM Observation of SS-FLC Samples

The textures of the FLC mixtures in 10- $\mu\text{m}$ -gap cells were observed using polarizing

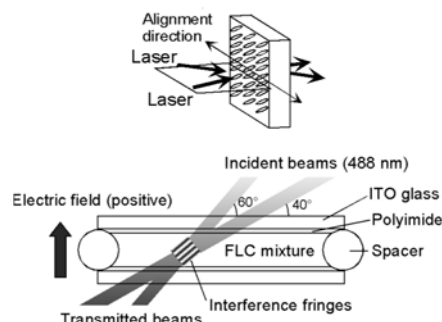


Fig. 5. Laser beam incidence condition and the structure of the LC cell.

optical microscopy (POM). The alignment of the FLC molecules is dominated not only by the properties of the FLCs but also by the affinity of FLC molecules with the alignment layer (polyimide coating). LC molecules interact with the alignment layer and form a homogeneous, anisotropic film in which the LC molecules are aligned in a specific direction. The fabrication of FLC cells involves the coating of ITO glass with the polyimide, rubbing treatment of the polyimide surface, and precise assembly of these glasses into a gap in a cell of only a few micrometers in width (Fig. 5). All of these processes affect the quality (homogeneity) of the surface-stabilized states, and the appropriate preparation conditions differ from FLC to FLC.

In this study, Hitachi Chemicals LX-1400 polyimide, used industrially in nematic LC displays, was chosen for the alignment layer. The thickness of the polyimide coating was set to 20-30 nm, and the surface of the polyimide was rubbed with a polyester velvet roll using a rubbing machine (RM-300/50, EHC Co. Ltd.) under specific conditions. Figures 6 and 7 show typical examples of textures observed in 3T-2MB samples and 3T-2OC samples under the polarizing microscope. As the concentration of the photoconductive chiral dopant increased, defects appeared in the texture. The 3T-2MB sample retained the uniformly aligned state with few defects for 3T-2MB concentrations below 8 wt.% (Fig. 6). However, the 3T-2OC sample retained the uniformly aligned state with few defects for 3T-2OC concentrations below 6 wt.% (Fig. 7). The spontaneous polarization in the 3T-2MB samples was smaller than 1 nC/cm<sup>2</sup>, while that in the 3T-2OC samples was about 5 nC/cm<sup>2</sup>. The smaller spontaneous polarization (thus, smaller intermolecular interactions) of the 3T-2MB sample might have contributed to the uniformity of the LC phase. It must be highlighted that a striped pattern was observed in the textures of the 3T-2MB samples (Fig. 6). This indicates that the 3T-2MB samples do not form a complete SS-state in the 10- $\mu$ m-gap cell. The striped pattern denotes the helical structure of the aligned LC molecules in the 10- $\mu$ m-gap cell. Zig-zag defects, which are typical defects in the SS-state (book shelf structure), are also observed in the texture (Fig. 6). It was considered that the FLC mixtures showed the SS-state at the area close to the glass surface and formed a helical structure around the centre of the thickness of the 10- $\mu$ m-gap cell.

### 3.2 Asymmetric energy exchange in FLC mixtures

The photorefractivity of the FLC mixtures was evaluated by two-beam coupling experiment. Figure 8 shows a typical example of the asymmetric energy exchange observed in a mixture of the base LC, 3T-2MB, and TNF at 25 °C with application of an electric field of 1 V/ $\mu$ m. Interference of the divided beams in the sample resulted in increased transmittance of one of the beams and decreased transmittance of the other beam. These transmittance characteristics were reversed when the polarity of the applied electric field was reversed. Asymmetric energy exchange was only observed when an electric field was applied, indicating that beam coupling was not caused by a thermal grating. About 40% of the energy of the laser beam L<sub>2</sub> was transferred to the L<sub>1</sub> beam.

In order to calculate the two-beam coupling gain coefficient, the diffraction condition needs to be correctly identified. The two possible diffraction conditions are the Bragg regime and the Raman-Nath regime, distinguished by the dimensionless parameter  $Q$ .<sup>2,3</sup>

$$Q=2\pi\lambda L/n\Lambda^2, \quad (1)$$

where  $\lambda$  is the wavelength of the laser,  $L$  is the interaction path length,  $n$  is the refractive index, and  $\Lambda$  is the grating spacing. The Bragg regime of optical diffraction

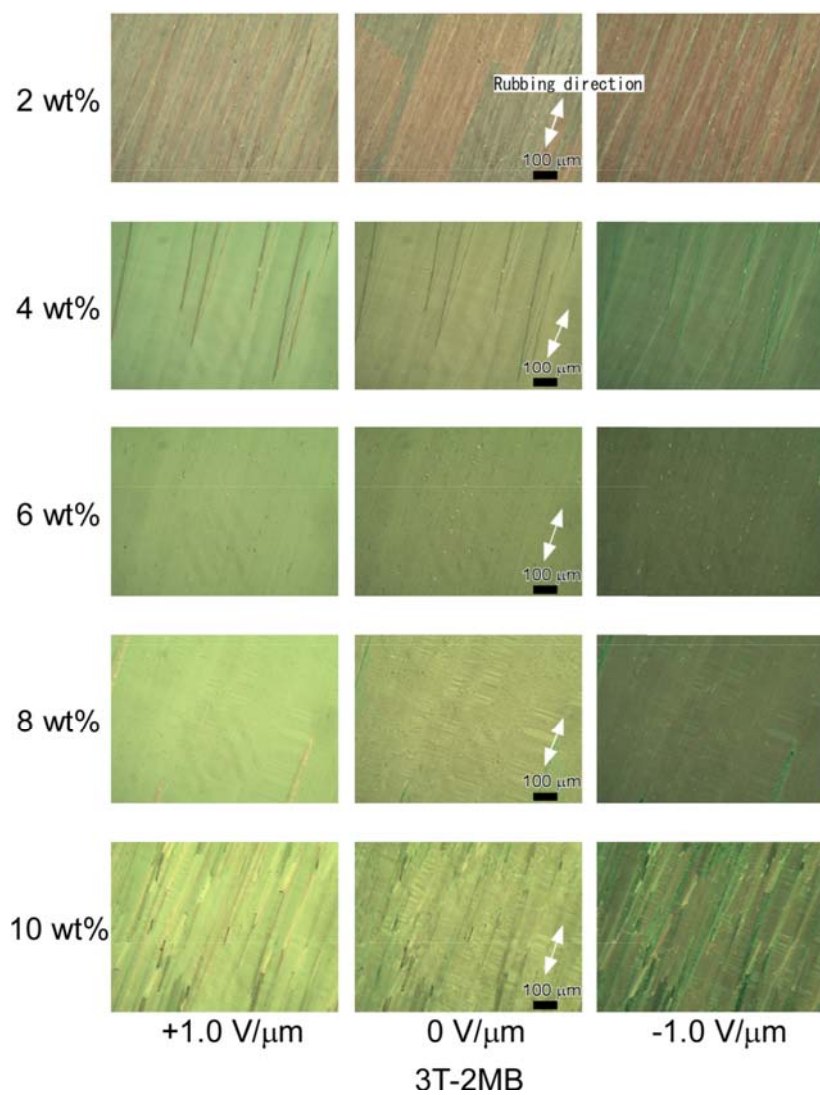


Fig. 6. Textures of FLC mixtures containing 3T-2MB in a 10- $\mu\text{m}$ -gap LC cell observed under a polarizing microscope. The strengths of the external electric field were +1.0 V/ $\mu\text{m}$ , 0 V/ $\mu\text{m}$ , and -1.0 V/ $\mu\text{m}$ . The direction of the applied electric field is shown in Fig. 5. The 3T-2MB concentrations were in the range of 2-10 wt.%, and 0.1 wt.% of TNF was added.

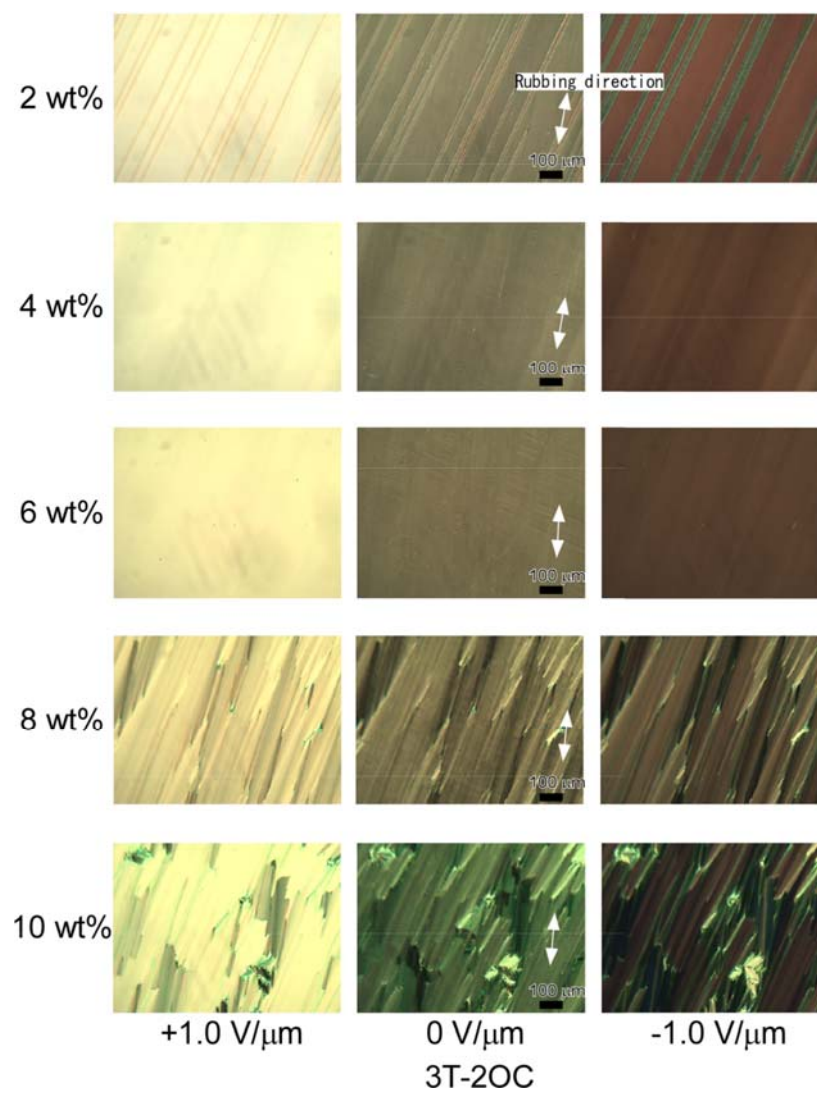


Fig. 7. Textures of FLC mixtures containing 3T-2OC in a 10- $\mu\text{m}$ -gap LC cell observed under a polarizing microscope. The strengths of the external electric field were +1.0 V/ $\mu\text{m}$ , 0 V/ $\mu\text{m}$ , and -1.0 V/ $\mu\text{m}$ . The direction of the applied electric field is shown in Fig. 5. The 3T-2OC concentrations were in the range of 2-10 wt.%, and 0.1 wt.% of TNF was added.

is defined as  $Q > 1$ , and excludes multiple scattering to produce only one order of diffraction of light. Conversely,  $Q < 1$  is defined as the Raman-Nath regime of optical diffraction, in which many orders of diffraction can be observed. A  $Q$  value greater than 10 is usually required to guarantee that diffraction occurs entirely in the Bragg regime. Under the present experimental conditions,  $Q$  is calculated to be 6.2. Therefore, the diffraction observed in this experiment occurs predominantly, but not entirely, in the Bragg regime, with a small Raman-Nath component. However, because higher-order diffraction was not observed, the two-beam coupling gain coefficient  $\Gamma$  was calculated assuming Bragg diffraction.<sup>2-6</sup>

$$\Gamma = \frac{1}{D} \ln \left( \frac{gm}{1+m-g} \right), \quad (2)$$

where  $D=L/\cos(\theta)$  is the interaction path for the signal beam ( $L$ =sample thickness,  $\theta$ =propagation angle of the signal beam in the sample),  $g$  is the ratio of the signal beam intensities behind the sample with and without a pump beam, and  $m$  is the ratio of the beam intensities (pump/signal) in front of the sample.

The gain coefficients of the samples were measured as a function of the applied electric field strength (Fig. 9). The gain coefficient was calculated to be  $1200 \text{ cm}^{-1}$  in the 10 wt.% sample with the application of only  $1.5 \text{ V}/\mu\text{m}$ . This gain coefficient is much higher than those of FLCs reported to date ( $800 \text{ cm}^{-1}$ ).<sup>1,11-15</sup> It was considered that a higher transparency of the LC mixture contributed to the high gain coefficient. The small electric field required to activate the photorefractive effect in FLCs is a great advantage for photorefractive devices. The response time decreased with increasing electric field strength due to the increased charge separation efficiency. The shortest formation time obtained was  $0.9 \text{ ms}$  for an external electric field of  $1.9 \text{ V}/\mu\text{m}$ . The large gain and fast response are advantageous for realizing optical devices such as real-time image amplifiers and accurate measurement

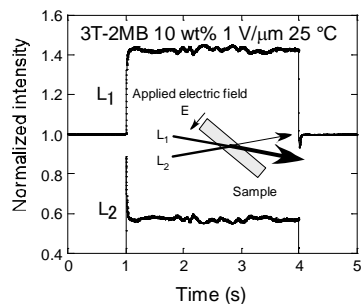


Fig. 8. Typical results of two-beam coupling experiments for a ternary mixture base LC, 3T-2MB, and TNF measured at  $25 \text{ }^\circ\text{C}$ . The pump beam  $L_2$  was incident at 1 s and closed at 4 s.

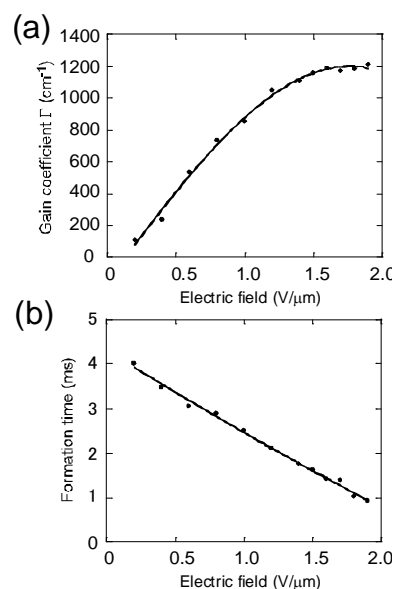


Fig. 9. (a) Electric field dependence of the gain coefficients for mixtures of the base LC, 3T-2MB (10 wt.%), and TNF (0.1 wt.%) measured at  $25 \text{ }^\circ\text{C}$ . (b) Refractive index grating formation times (response time) for mixtures of the base LC, 3T-2MB (10 wt.%), and TNF (0.1 wt.%) measured at  $25 \text{ }^\circ\text{C}$ .

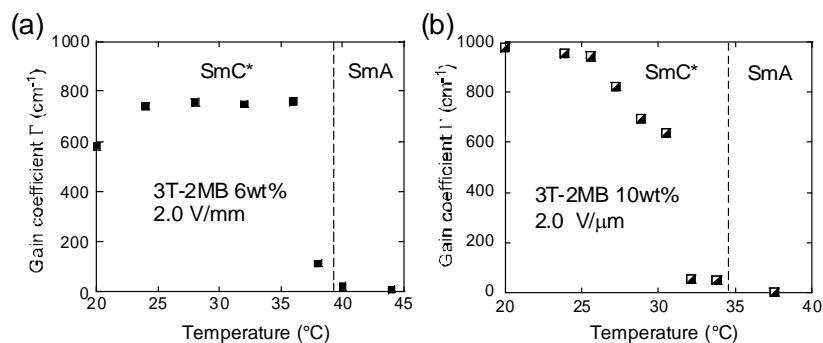


Fig. 10. Temperature dependence of gain coefficients and formation times. The concentration of 3T-2MB was (a) 6 wt.% and (b) 10 wt.%.

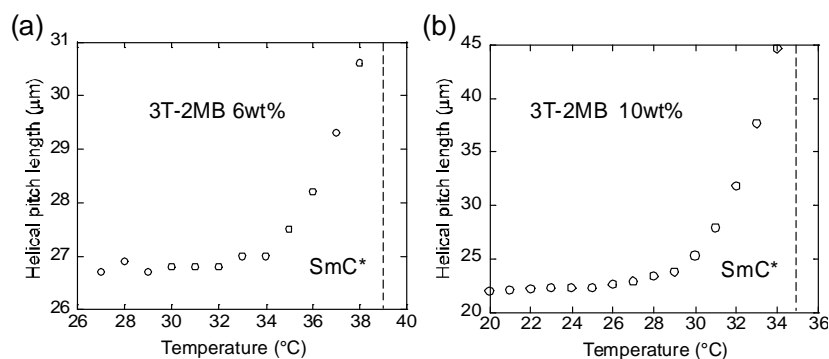


Fig. 11. Temperature dependence of helical pitch lengths. The concentration of 3T-2MB was (a) 6 wt.% and (b) 10 wt.%.

devices.<sup>2,3,18</sup>

### 3.3 Temperature dependence of the photorefractive effect of FLCs

The temperature dependence of the gain coefficient of the 3T-2MB samples is shown in Fig. 10. Asymmetric energy exchange was observed at temperatures below the SmC\*-SmA phase transition temperature. The helical pitch of the 3T-2MB samples observed in the polarizing microscope is plotted as a function of temperature in Fig. 11. Similarly, the helical pitch diverged when the temperature approached the phase transition temperature. In our previous study, the asymmetric energy exchange in an FLC sample was observed only in the temperature range in which the sample exhibits spontaneous polarization. Thus, asymmetric energy exchange was observed only in the temperature range in which the sample exhibits ferroelectric properties (SmC\* phase).

### 3.4 Effect of the concentration of photoconductive chiral dopant

The gain coefficient of the samples with different 3T-2MB concentrations is plotted as a function of the magnitude of the external electric field in Fig. 12. The gain coefficient increased with the strength of the external electric field up to 0.2-0.6 V/μm and reached a constant value. It is considered that the decrease in the gain coefficient

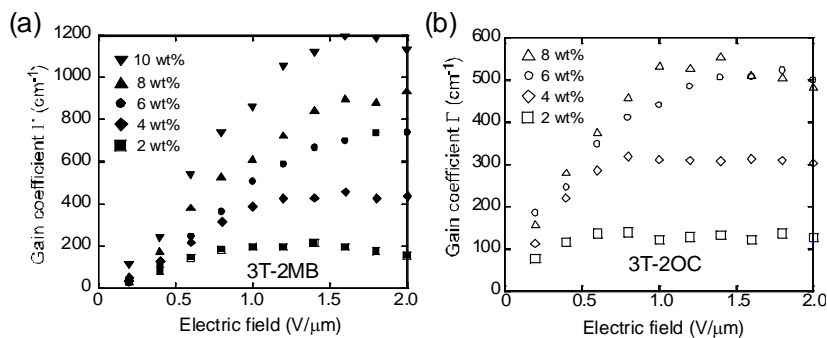


Fig. 12. Electric field dependence of the gain coefficients of the mixtures of the base LC, 3T-2MB, and TNF (0.1 wt.%) measured at 25 °C. The concentrations of 3T-2MB were in the range of 2-10 wt.%.

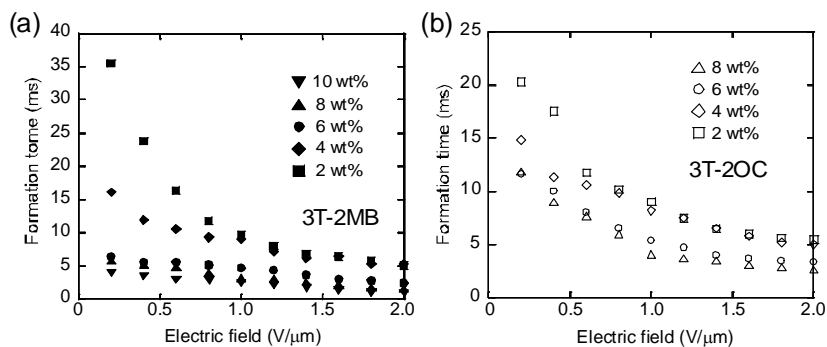


Fig. 13. Refractive index grating formation time (response time) of the mixtures of the base LC, 3T-2MB, and TNF (0.1 wt.%) measured at 25 °C. The 3T-2MB concentrations were in the range of 2-10 wt.%.

at a high external electric field is due to the realignment of the FLC molecules being restricted because the strength of the external electric field exceeded that of the internal electric field. As the concentration of the photoconductive chiral dopants increased, so did the gain coefficient. This may be due to increased density of charge carriers in the FLC medium and an increase in the magnitude of spontaneous polarization (Ps). The magnitude of the gain coefficient was independent of the concentration of TNF. It was considered that conduction based on a hopping mechanism occurred. In this case, TNF acts as just the electron acceptor that introduces electron holes into the photoconductive chiral dopant. Since the molecular weight of photoconductive chiral dopant is not very different from that of the LC molecules, approximately four photoconductive dopant molecules are dispersed in 96 LC molecules. A cube wherein each side includes 5 LC molecules contains 125 LC molecules. Thus, the average distance between the photoconductive chiral dopant molecules in the LC phase is less than 3 LC molecules. In this case, charge transport based on a hopping mechanism might not be impossible. However, a more detailed understanding of the charge transport mechanism in the dye-doped FLC medium requires further investigation. The gain coefficient was calculated to be 1200 cm<sup>-1</sup> in the 10 wt.% 3T-2MB sample with the application of only 1.6 V/μm. This gain coefficient is twice as high as that of the 3T-2OC sample.

The response time of the samples is plotted as a function of the magnitude of the external electric field in Fig. 13. The response time decreased with increasing electric field strength due to increased charge separation efficiency. The shortest formation time of 0.93 ms was obtained in the 10 wt.% 3T-2MB sample with the application of 2.0 V/ $\mu\text{m}$ . This response time was shorter than that of the 3T-2OC samples. Although the magnitude of the spontaneous polarization in the 3T-2OC samples (5 nC/cm<sup>2</sup>) is higher than that in the 3T-2MB sample (< 1 nC/cm<sup>2</sup>), the gain coefficient and response speed are higher for the 3T-2OC sample. This indicates that transparency is more important for the photorefractive effect of FLCs than the magnitude of spontaneous polarization.

### 3.5 Dynamic amplification of optical image in photorefractive FLCs

Optical image amplification was demonstrated in this work (Fig. 14). A computer-generated image was displayed on a spatial light modulator (SLM) and a 473 nm DPSS laser beam was irradiated. The laser beam containing the image (signal beam) was transmitted through the FLC sample and monitored by a CCD camera. When the pump beam (a beam divided from the signal beam before SLM) was incident to the FLC sample and interfered with the signal beam, the signal was amplified through asymmetric energy exchange. The crossing angle of the beams at 15° yielded the largest amplification and the best contrast. The intensities of the optical signal beam with and without the pump beam are shown in Fig. 15. The intensity of the signal beam was amplified 6-fold compared to that without the pump

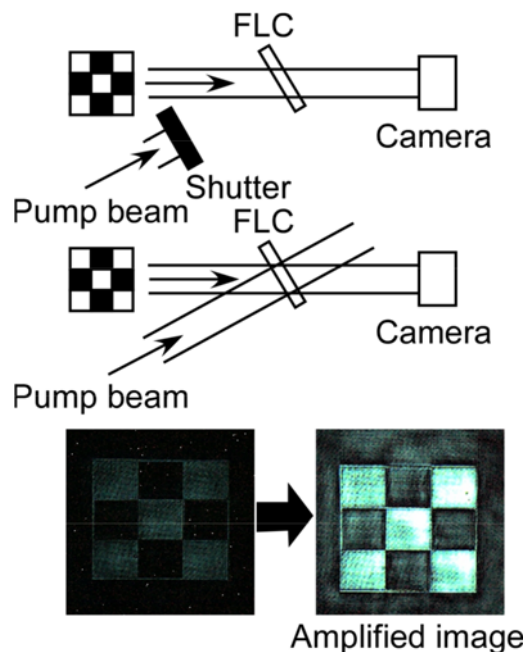


Fig. 14. Optical image amplification experiment. A computer-generated image was displayed on the SLM. The SLM modulated the object beam (473 nm), which was irradiated on the FLC sample and interfered with the pump beam. The Image transmitted through the FLC sample (3T-2MB, 10 wt.%) was monitored by a CCD camera.

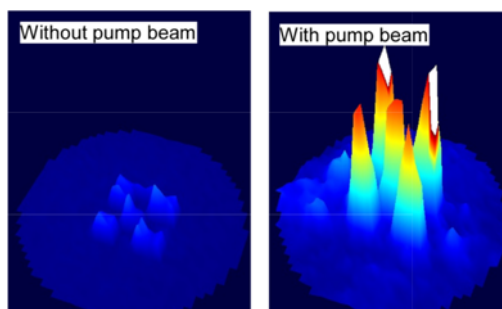


Fig. 15. Signal beam intensities without and with the pump beam.

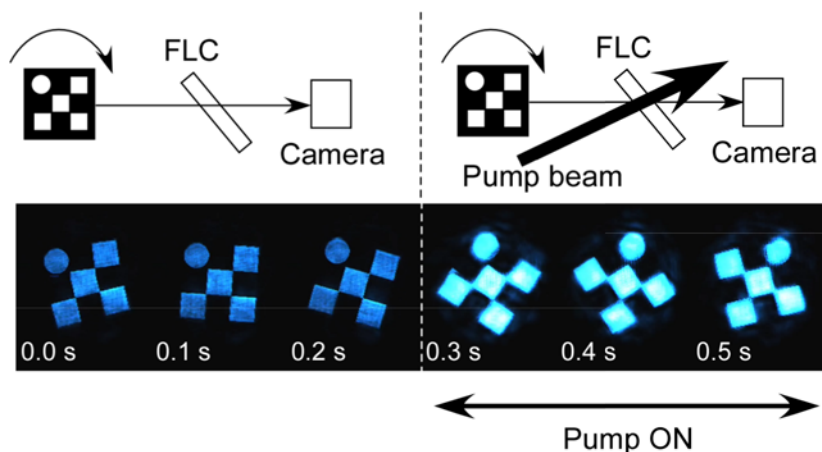


Fig. 16. Optical image amplification experiment. A computer-generated animation was displayed on the SLM. The SLM modulated the object beam (473 nm), which was irradiated on the FLC sample, and interfered with the reference beam. The image transmitted through the FLC sample (3T-2MB, 10 wt.%) was monitored by a CCD camera.

beam.

A computer-generated animation was displayed on the SLM. The frame rate was 30 fps. A 473 nm beam was irradiated on the SLM and the reflected beam was incident on the FLC sample. A pump beam interfered with the beam from the SLM in the FLC sample. A laser beam containing the moving image of the animation was amplified by the incident pump beam (Fig. 16). This result shows that the response of the photorefractive FLC was fast enough to amplify the optical image in real time. If a typical photorefractive polymer with a response time of  $\sim 100$  ms is used in place of the FLC sample, the amplification would not occur. In that case, although a still image can be amplified, the intensity of the image would be weakened to the original magnitude when the image starts to move at a video rate.

#### 4. Conclusion

The photorefractivity of photoconductive FLC mixtures containing photoconductive chiral dopants was investigated. Relatively large gain coefficients higher than  $1200$   $\text{cm}^{-1}$  with a response time (refractive index grating formation time) of 1 ms were obtained under application of only  $1.5$   $\text{V}/\mu\text{m}$  in the SS-state of a FLC mixture. This response time is sufficiently short to realize real-time dynamic holograms. Because the molecular shape of the terthiophene-type photoconductive chiral dopants is similar to that of the base LC molecules, the miscibility with the base LC is high. FLC mixtures containing the photoconductive chiral dopants exhibited high gain coefficient and first response, making them useful for photorefractive devices. Real-time dynamic amplification of the optical image signal using the photorefractive ferroelectric liquid crystal was demonstrated.

#### References

a Department of Chemistry, Faculty of Science, Tokyo University of Science, 1-3

Kagurazaka, Shinjuku-ku, Tokyo 162-8601, Japan; E-mail: sasaki@rs.kagu.tus.ac.jp

- 1 T. Sasaki, M. Ikegami, T. Abe, D. Miyazaki, S. Kajikawa and Y. Naka, *Appl. Phys. Lett.* 102, 063306, 1-4 (2013).
- 5 2 L. Solymar, J. D. Webb, and Grunnet-Jepsen, A. *The Physics and Applications of Photorefractive Materials* (Oxford: New York, 1996).
- 3 P. Yeh, *Introduction to Photorefractive Nonlinear Optics* (John Wiley: New York, 1993).
- 4 W. E. Moerner, and S. M. Silence, *Chem. Rev.* 94, 127-155 (1994).
- 10 5 B. Kippelen, and N. Peyghambarian, *Advances in Polymer Science, Polymers for Photonics Applications II* 87-156 (Springer, 2002).
- 6 O. Ostroverkhova, and W. E. Moerner, *Chem. Rev.* 104, 3267-3314 (2004).
- 7 T. Sasaki, *Polymer Journal*, 37, 797-812 (2005).
- 8 S. Tay, P. A. Blanche, R. Voorakaranam, A. V. Tunc, W. Lin, S. Rokutanda, T. Gu, D. Flores, P. Wang, G. Li, P. Hilarie, J. Thomas, R. A. Norwood, M. Yamamoto, and N. Peyghambarian, *Nature*, 451, 694-698 (2008).
- 15 9 P. A. Blanche, A. Bablumian, R. Voorakaranam, C. Christenson, W. Lin, T. Gu, D. Flores, P. Wang, W. Y. Hsieh, M. Kathaperumal, B. Rachwal, O. Siddiqui, J. Thomas, R. A. Norwood, M. Yamamoto, and N. Peyghambarian, *Nature*, 468, 80-83 (2010).
- 20 10 H. Ono and N. Kawatsuki, *Opt. Lett.*, 22, 1144-1146 (1997).
- 11 T. Sasaki, D. Miyazaki, K. Akaike, M. Ikegami and Y. Naka, *J. Mater. Chem.*, 21, 8678-8686 (2011).
- 12 G. P. Wiederrecht, B. A. Yoon, and M. R. Wasielewski, *Adv. Materials* 12, 1533-1536 (2000).
- 25 13 M. Talarico, R. Termine, P. Prus, G. Barberio, D. Pucci, M. Ghedini, A. Goelemme, *Mol. Cryst. Liq. Cryst.* 429, 65-76 (2005).
- 14 M. Talarico and A. Goelemme, *Nature Mater.* 5, 185-188 (2006).
- 15 T. Sasaki, *Chem. Rec.* 6, 43-51 (2006).
- 30 16 K. Sarp and A. A. Handschy, *Mol. Cryst. Liq. Cryst.* 165, 439-509 (1988).
- 17 P. Oswald and P. Pieranski *Smectic and Columnar Liquid Crystals* (Taylor & Francis: New York, 2006)
- 18 N. Koukourakis, T. Abdelwahab, M. Y. Li, H. Höpfner, Y. W. Lai, E. Darakis, C. Brenner, N. C. Gerhardt, and M. R. Hofmann, *Opt. Express* 19, 22004-22023 (2011).
- 35